Average energy per C−beta interaction of 9766 PDB chains
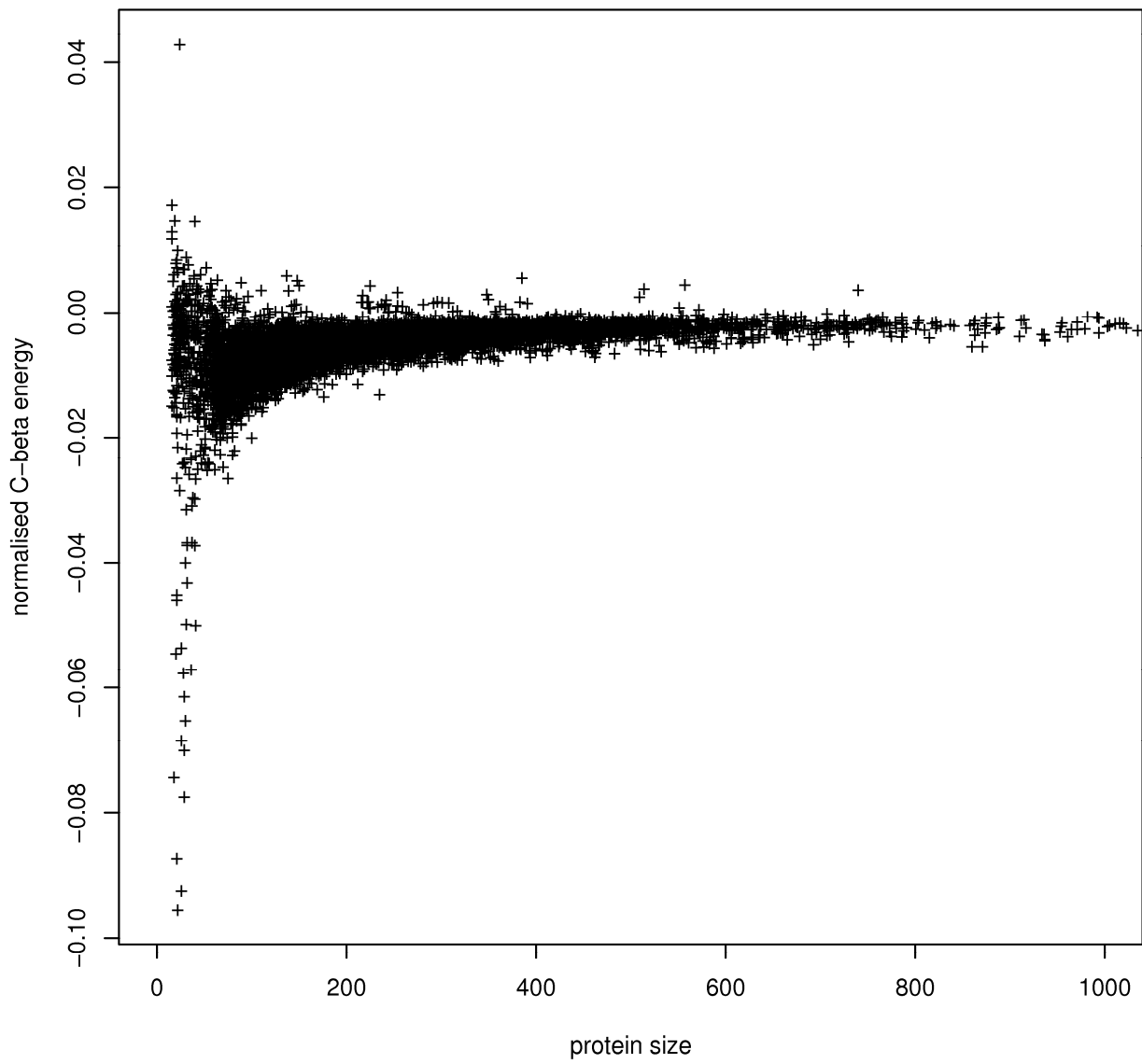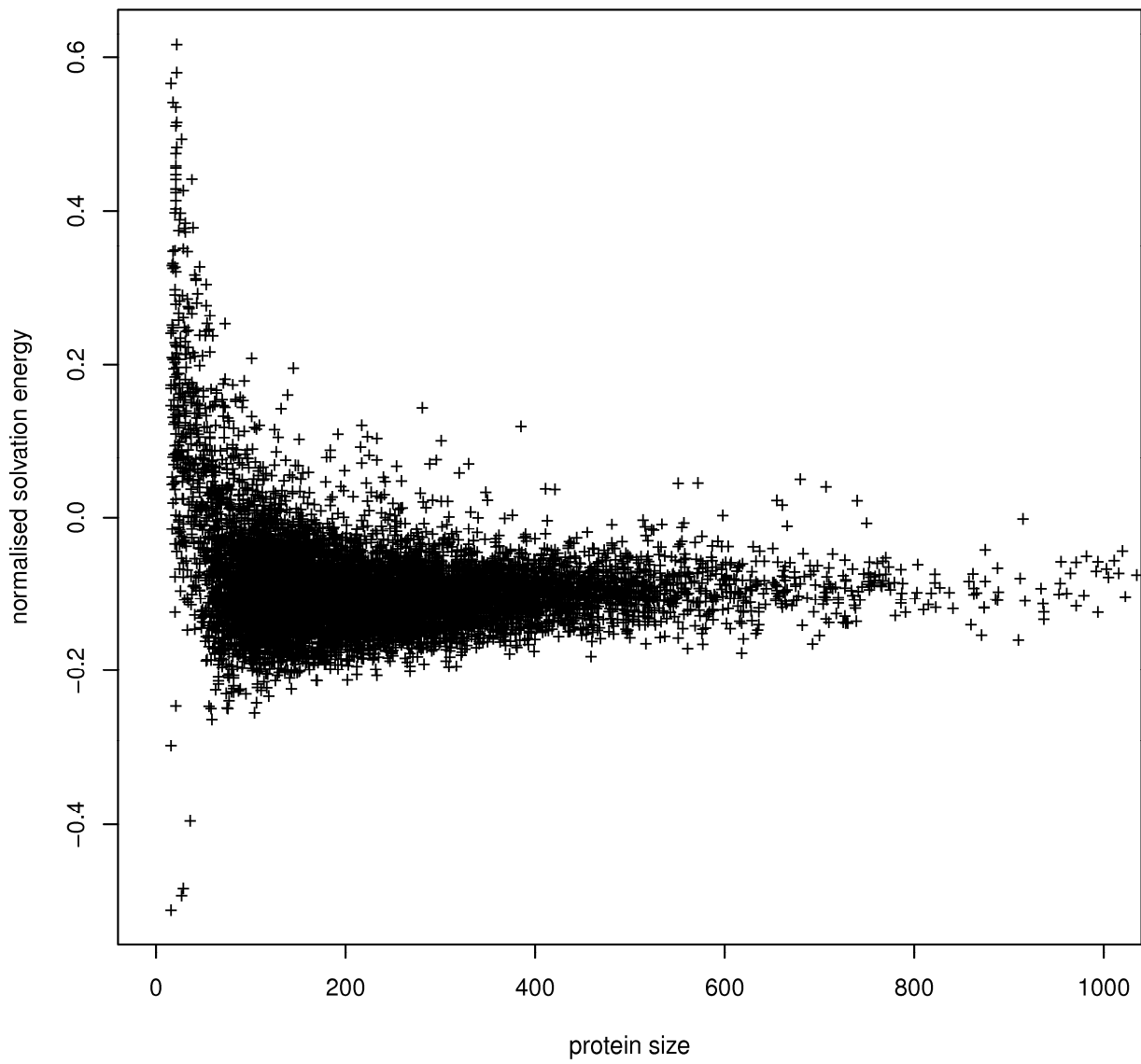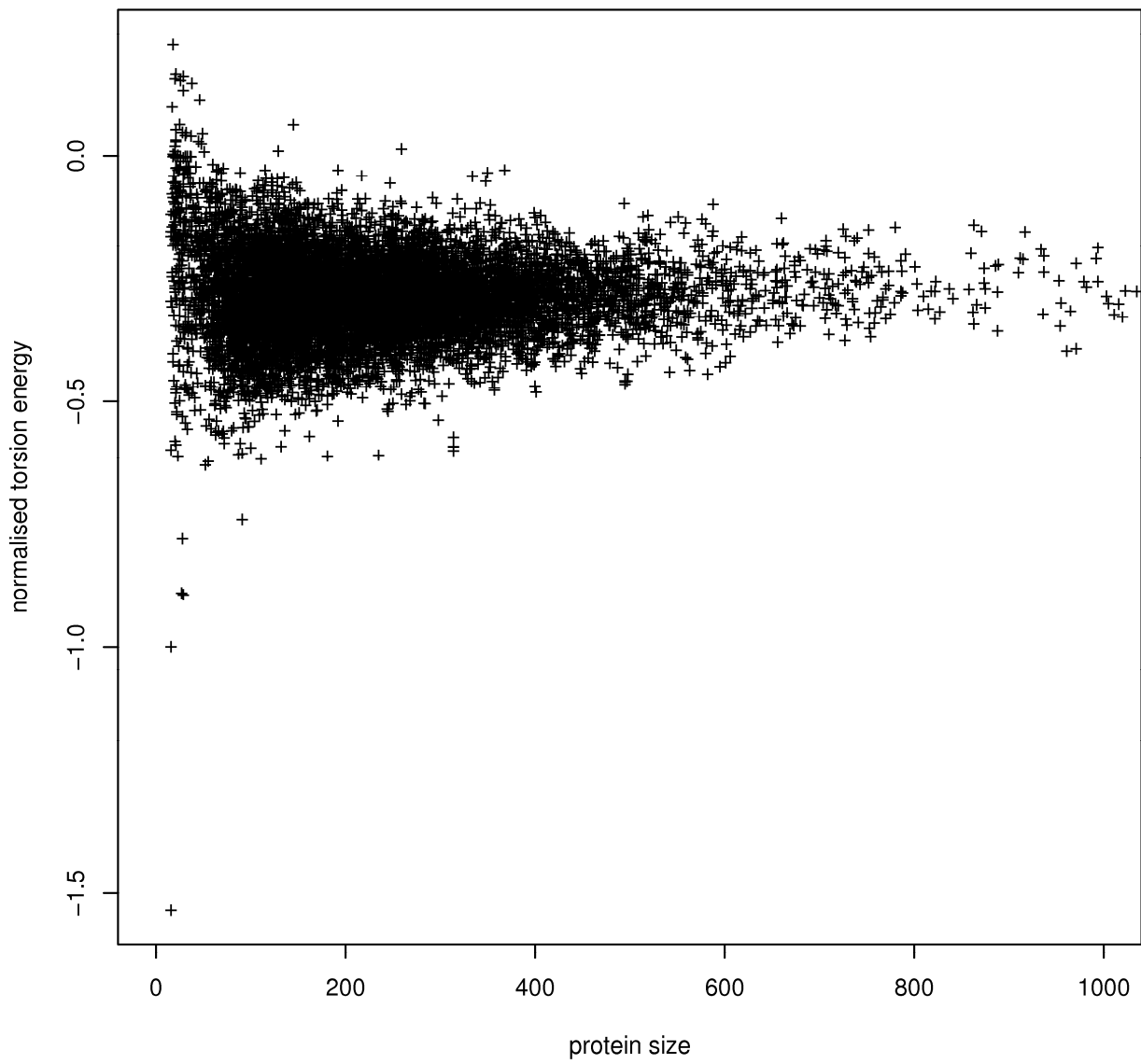
Figure S1: Normalized residue-level interaction energy for the PDB reference set.

Average solvation energy of 9766 PDB chains

Figure S2: Average residue solvation energy observed in the PDB reference set.

Figure S3: Average torsion angle energy observed in the PDB reference set.

Table S1: 18 chains excluded from the *PDB reference set* with a QMEAN Z-score of more than 3 standard deviations (all solved by X-ray diffraction).

| PDB	chain	size	Keywords	Resoluition	Zscore
1AYM	1	285	HUMAN RHINOVIRUS 16 COAT PROTEIN	2.15	-3.07
1B35	C	282	CRICKET PARALYSIS VIRUS, VP3	2.40	-3.29
1EGI	A	129	MACROPHAGE MANNOSE RECEPTOR	2.30	-3.24
1INP	A	400	INOSITOL POLYPHOSPHATE 1-PHOSPHATASE	2.30	-3.01
1LJ2	A	106	NONSTRUCTURAL RNA-BINDING PROTEIN 34	2.38	-3.08
1LPB	A	85	COLIPASE	2.46	-3.41
1N1C	A	199	TorA specific chaperone	2.40	-3.63
1PYA	A	81	PYRUVOYL-DEPENDENT HISTIDINE DECARBOXYLASE	2.50	-3.29
1WDC	A	64	SCALLOP MYOSIN	2.00	-3.03
2B1Y	A	101	hypothetical protein Atu1913	1.80	-3.12
2BUK	A	184	SATELLITE TABACCO NECROSIS VIRUS COAT PROTEIN	2.45	-3.44
2DXC	B	152	Thiocyanate hydrolase subunit beta	1.90	-3.25
2I15	A	122	Hypothetical protein MG296 homolog	2.40	-3.67
2Q97	T	109	Toxofilin	2.50	-3.30
2V0X	A	195	LAMINA-ASSOCIATED POLYPEPTIDE	2.20	-3.13
2VTY	A	144	VACCINIA VIRUS ANTI-APOPTOTIC F1L	2.10	-3.38
2ZIB	A	130	Type II antifreeze protein	1.34	-3.26
3FS3	A	197	Malaria parasite Nucleosome Assembly Protein (NAP)	2.30	-3.00

Table S2: Outlier peptides of very high and low normalized all-atom energy observed in a non-redundant dataset of 9766 proteins solved by X-ray crystallography. The low energy of the three peptides can be partly explained by an over-representation of disulfide bridges: heptidin has four SS-bonds, endothelin-1 two and relaxin one. The per-interaction energies averaged over the atoms of bonded cysteins in these peptides range from -1.34 to -0.83 which is roughly a factor 200 higher than the average interaction values in globular proteins. The average energy per interaction in the PDB referece set converges to an value of -0.0058+/-0.0017 (see Fig. 1). Relaxin has, beside the disulfide bond, a pronounced hydrophobic core appearing as four pairs of hydrophobic residues with average interaction energy below -0.4 on the list of predicted low-energy interactions.

PDB id	chain	size	# SS-bonds	description	normalised all-atom energy
3H0T	C	22	4	Hepcidin	-0.090
1EDN	A	21	2	Endothelin-1	-0.040
6RLX	A	24	1	Relaxin	-0.039
2VQE	U	24	0	30S ribosomal protein THX	0.022
1UVQ	C	20	0	Hypocretin peptide in MHC class II	0.022
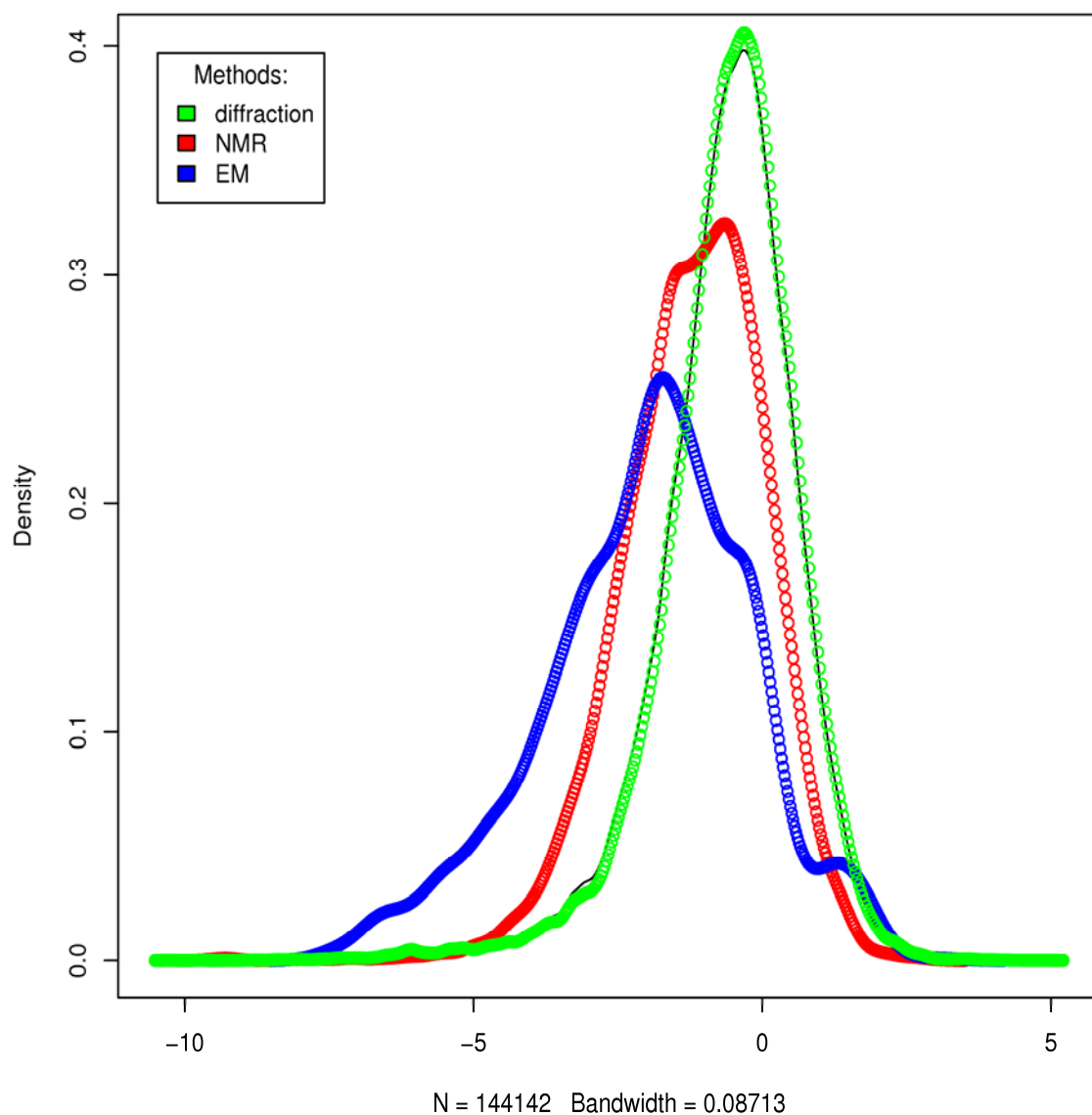
Figure S4: QMEAN Z-score analysis of 144,142 chains from the SwissModel template library which is based on the current PDB. Three density plots are shown for QMEAN Z-scores of proteins solved by different methods: X-ray crystallography (green), NMR spectroscopy (red), electron microscopy (blue).
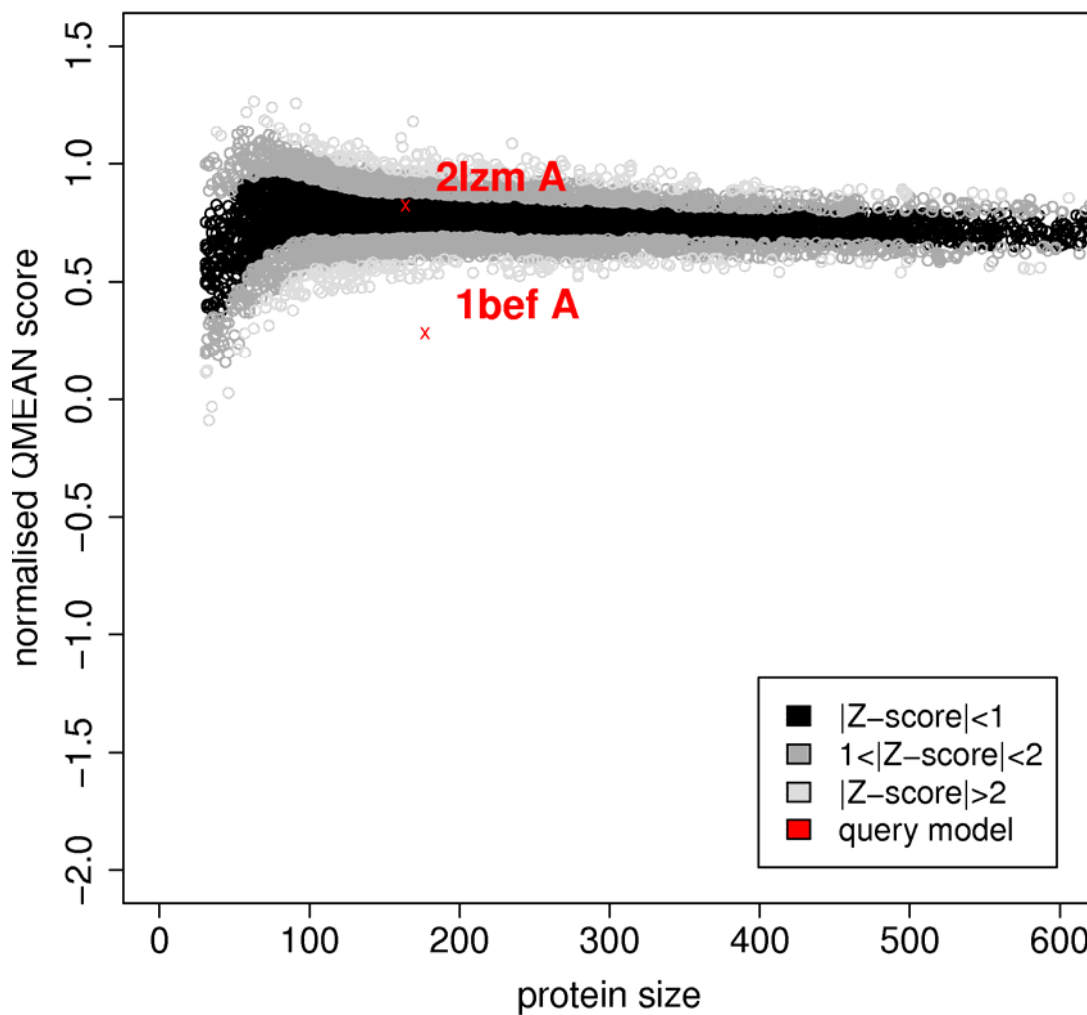
Figure S5: Visualisation of the QMEAN score of two selected protein structures with respect to proteins from the *PDB reference set*: T4 a bacteriophage lysozyme (2lzm, chain A) and a structure of the Dengue virus NS3 serine protease (1bef, chain A). While the structure of T4 bacteriophage lysozyme exhibits scores as expected for a high-quality experimental structure of this size, the scores for 1bef indicates that the features of this structure deviate significantly from expectation (**Table 2**). Compare to ProSA outputs in **Figure S6**.
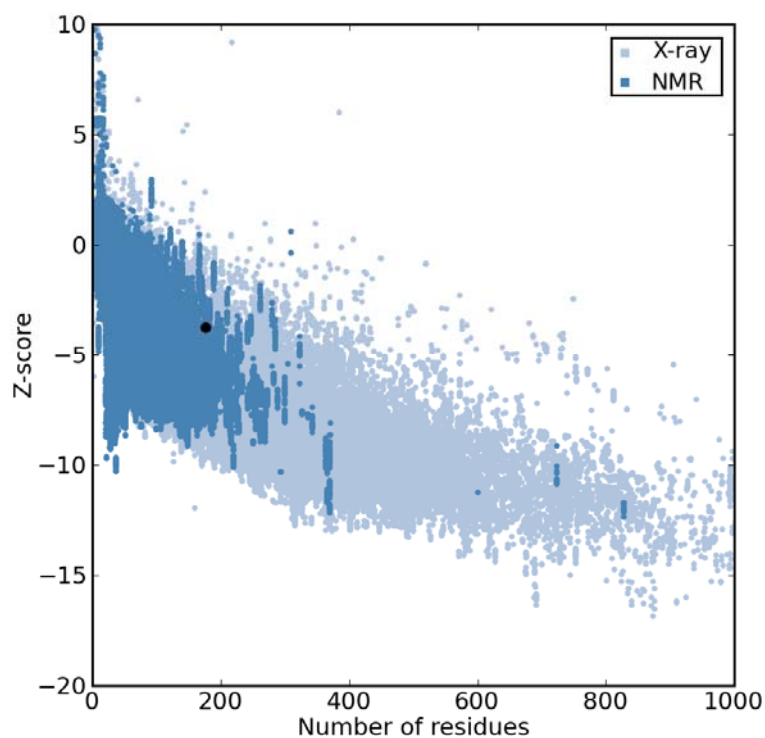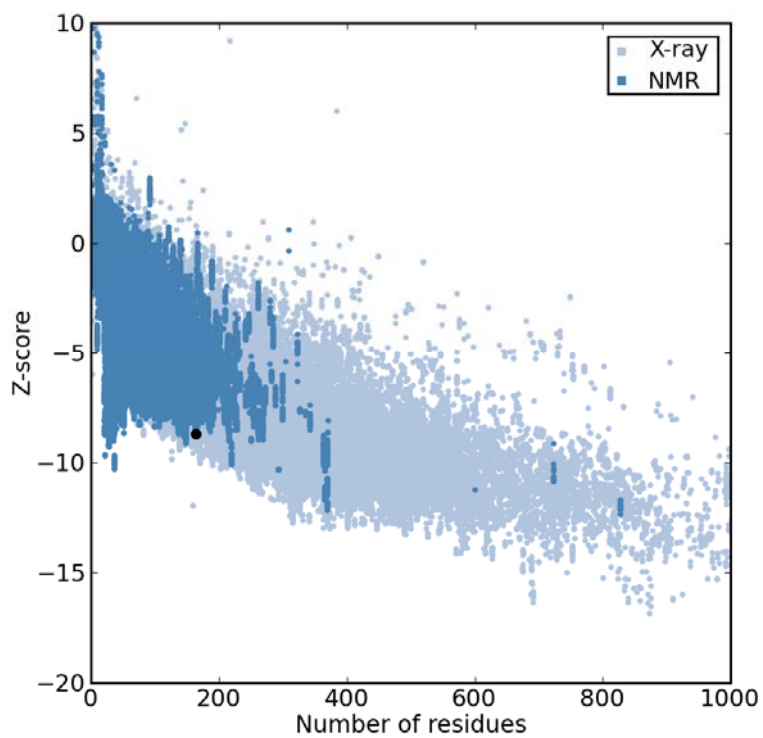
Figure S6: Visualisation of the ProSA Z-score of T4 a bacteriophage lysozyme (*upper plot:* 2lzm, chain A, ProSA **Z-score=-8.7**) and a structure of the Dengue virus NS3 serine protease (*lower plot:* 1bef, chain A, ProSA **Z-score=-3.74**).

Table S3: QMEAN Z-score analysis of all structures submitted to the PDB by the group of K.H.M Murthy. The University of Alabama at Birmingham has requested the PDB to retract these structures – a fraction of them has already been removed.

PDB id	chain	size	Zscore_QMEANnorm	Zscore_Cbeta	Zscore_all_atom	Zscore_solvation	Zscore_torsion
1bef	A	177	-5.5	-3.4	-3.6	-2.7	-4.1
1cmw	A	817	-1.1	0.2	0.1	0.5	-1.6
1df9	A	177	-5.0	-3.2	-3.4	-2.6	-3.5
1df9	B	177	-5.7	-3.1	-3.4	-2.7	-4.3
1df9	C	72	-1.7	1.2	-1.4	0.2	-1.9
1g40	A	243	-4.1	-3.1	-2.9	-1.9	-3.3
1g40	B	243	-4.5	-3.0	-2.9	-2.0	-3.8
1g44	A	223	-3.8	-2.9	-2.7	-2.1	-2.6
1g44	B	231	-4.0	-3.1	-2.8	-2.1	-3.0
1g44	C	228	-3.9	-3.1	-2.8	-2.0	-2.8
1l6l	A	74	-3.2	-2.6	-2.7	-2.0	-2.3
1l6l	B	74	-3.0	-1.4	-1.4	-1.9	-2.7
1l6l	C	76	-2.7	-1.3	-1.1	-2.1	-2.3
1l6l	D	74	-2.9	-1.2	-1.3	-2.0	-2.6
1l6l	E	72	-3.2	-1.2	-1.2	-2.6	-2.6
1l6l	F	75	-2.5	-1.9	-1.4	-1.8	-2.1
1l6l	G	74	-2.7	-1.1	-1.3	-2.0	-2.2
1l6l	H	74	-2.6	-1.3	-1.3	-1.8	-2.3
1l6l	I	73	-3.3	-1.5	-2.0	-2.4	-2.4
1l6l	J	74	-2.7	-1.5	-1.3	-1.8	-2.4
1l6l	K	74	-2.6	-1.3	-1.6	-2.0	-1.8
1l6l	L	74	-3.0	-1.5	-1.6	-2.4	-2.1
1l6l	M	76	-2.9	-1.3	-1.1	-2.4	-2.4
1l6l	N	76	-3.3	-1.5	-1.6	-2.7	-2.3
1l6l	P	73	-3.0	-1.4	-1.7	-2.0	-2.4
1l6l	Q	73	-2.8	-1.7	-1.6	-2.3	-2.0
1l6l	S	74	-3.1	-2.5	-2.7	-2.0	-2.2
1l6l	T	74	-2.9	-1.6	-1.5	-2.0	-2.5
1l6l	U	76	-2.9	-1.0	-1.1	-2.0	-2.5
1l6l	V	75	-3.0	-1.4	-1.5	-2.0	-2.5
1l6l	W	73	-3.0	-1.1	-1.2	-2.2	-2.5
1l6l	X	75	-2.8	-1.8	-1.7	-1.9	-2.2
1l6l	Y	74	-2.8	-1.2	-1.3	-1.9	-2.4
1l6l	Z	72	-3.0	-1.0	-1.4	-1.9	-2.6
1l6l	1	73	-3.4	-1.5	-2.2	-2.6	-2.2
1l6l	2	73	-3.0	-1.7	-1.5	-2.2	-2.5
1l6l	3	73	-3.2	-1.3	-1.7	-2.6	-2.1
1l6l	4	74	-3.0	-1.8	-2.1	-2.6	-1.7
1l6l	5	75	-2.9	-1.5	-0.9	-2.6	-2.3
1l6l	6	75	-3.7	-1.8	-1.7	-3.4	-2.4
1l6l	7	70	-3.2	-1.2	-2.1	-2.2	-2.2
1l6l	8	74	-3.1	-1.1	-1.3	-2.1	-2.7
1rid	A	244	-4.6	-2.7	-2.9	-2.4	-3.7
1rid	B	244	-4.5	-2.8	-3.0	-2.4	-3.4
1y8e	A	244	-4.1	-2.4	-2.7	-2.2	-3.1
1y8e	B	243	-4.9	-2.6	-3.0	-2.7	-3.7
2a01	A	243	-1.7	-0.2	1.7	-1.0	-2.4
2a01	B	243	-2.1	0.4	1.6	-0.8	-2.9
2a01	C	243	-2.0	-0.1	1.7	-0.8	-2.9
2hr0	A	641	-0.5	0.3	0.1	-0.7	-0.2
2hr0	B	908	-2.5	0.4	0.5	-0.4	-2.8
2ou1	A	72	-2.9	-1.8	-1.3	-2.3	-2.4
2ou1	B	71	-3.0	-1.9	-1.7	-2.3	-2.2
2ou1	C	73	-2.7	-1.6	-1.2	-2.1	-2.3
2ou1	D	72	-3.2	-1.8	-1.5	-1.9	-3.0
2ou1	E	72	-2.7	-1.8	-1.2	-2.3	-2.1
2ou1	F	71	-2.9	-1.9	-1.8	-2.3	-2.1
2ou1	G	73	-2.9	-1.6	-1.2	-2.2	-2.4
2ou1	H	72	-3.1	-1.8	-1.4	-1.9	-3.0
2ou1	I	72	-2.9	-1.8	-1.3	-2.3	-2.4
2ou1	J	70	-2.9	-1.8	-1.6	-2.1	-2.3
2ou1	K	73	-2.7	-1.6	-1.2	-2.1	-2.2
2ou1	L	72	-3.2	-1.9	-1.5	-1.9	-3.1
2qid	A	177	-5.0	-3.2	-3.4	-2.6	-3.5
2qid	B	177	-5.7	-3.1	-3.4	-2.7	-4.3
2qid	C	72	-1.7	1.2	-1.4	0.2	-1.9

Table S4: Analysis of individual chains of the PDB (only structures solved by X-ray crystallography): list of outliers (grouped by chains) with QMEAN Z-score deviating by more than 5 standard deviations which are neither membrane proteins nor ribosomal proteins.

| PDB ID	Chain	Description	Resolution
1C8B	A,B	CRYSTAL STRUCTURE OF A NOVEL GERMINATION PROTEASE FROM SPORES OF BACILLUS MEGATERIUM: STRUCTURAL REARRANGEMENTS AND ZYMOGEN ACTIVATION	3.00
1DNV	A	PARVOVIRUS (DENSOVIRUS) FROM GALLERIA MELLONELLA	3.60
1FFX	A,B,C,D,E	TUBULIN:STATHMIN-LIKE DOMAIN COMPLEX	3.95
1FZP	B,D	CRYSTAL STRUCTURES OF SARA: A PLEIOTROPIC REGULATOR OF VIRULENCE GENES IN S. AUREUS	2.95
1KEN	A-F,H,L,T,U	INFLUENZA VIRUS HEMAGGLUTININ COMPLEXED WITH AN ANTIBODY THAT PREVENTS THE HEMAGGLUTININ LOW PH FUSOGENIC TRANSITION	3.50
1KTK	A,B,C,D,E,F	Complex of Streptococcal pyrogenic enterotoxin C (SpeC) with a human T cell receptor beta chain (Vbeta2.1)	3.00
1LDK	A,B,C,D,E	Structure of the Cul1-Rbx1-Skp1-F boxSkp2 SCF Ubiquitin Ligase Complex	3.10
1LQV	A,B,C,D	Crystal structure of the Endothelial protein C receptor with phospholipid in the groove in complex with Gla domain of protein C.	1.60
1N7D	A	Extracellular domain of the LDL receptor	3.70
1OAU	H-O	FV STRUCTURE OF THE IGE SPE-7 IN COMPLEX WITH DNP-SER (IMMUNISING HAPTEN)	1.80
1QTJ	A,B	CRYSTAL STRUCTURE OF LIMULUS POLYPHEMUS SAP	3.00
1S58	A	The structure of B19 parvovirus capsid	3.50
1TNV	A,B,C	CRYSTAL STRUCTURAL ANALYSIS OF TOBACCO NECROSIS VIRUS (TNV) AT 5 ANGSTROMS RESOLUTION	5.00
1TUB	A,B	TUBULIN ALPHA-BETA DIMER, ELECTRON DIFFRACTION	3.70
1W8X	A-P	STRUCTURAL ANALYSIS OF PRD1	4.20
1XGF	A,B	Backbone Structure of COCOSIN, an 11S storage protein from cocos nucifera	2.61
1XUP	O,X	ENTEROCOCCUS CASSELIFLAVUS GLYCEROL KINASE COMPLEXED WITH GLYCEROL	2.75
1Z56	A,B,C,F,G,I,J	Co-Crystal Structure of Lif1p-Lig4p	3.92
2BF1	A	STRUCTURE OF AN UNLIGANDED AND FULLY-GLYCOSYLATED SIV GP120 ENVELOPE GLYCOPROTEIN	4.00
2BFU	L,S	X-RAY STRUCTURE OF CPMV TOP COMPONENT	4.00
2FK0	A-R	Crystal Structure of a H5N1 influenza virus hemagglutinin.	2.95
2GLS	A-L	REFINED ATOMIC MODEL OF GLUTAMINE SYNTHETASE AT 3.5 ANGSTROMS RESOLUTION	3.50
2GTT	A-V	Crystal structure of the rabies virus nucleoprotein-RNA complex	3.49
2H8A	A	Structure of Microsomal Glutathione Transferase 1 in Complex with Glutathione	3.20
2HOD	A-L	Crystal Structure of Fragment D from Human Fibrinogen Complexed with Gly-hydroxyPro-Arg-Pro-amide	2.90
2IJZ	A-L	Crystal structure of aminopeptidase	3.00
2INY	A	Nanoporous Crystals of Chicken Embryo Lethal Orphan (CELO) Adenovirus Major Coat Protein, Hexon	3.90
2NN6	A-I	Structure of the human RNA exosome composed of Rrp41, Rrp45, Rrp46, Rrp43, Mtr3, Rrp42, Csl4, Rrp4, and Rrp40	3.35
2PFF	A-I	Structural Insights of Yeast Fatty Acid Synthase	4.00
2PGK	A	THE USE OF PHASE COMBINATION IN THE REFINEMENT OF PHOSPHOGLYCERATE KINASE AT 2.5 ANGSTROMS RESOLUTION	3.00
2QZV	A,B	Draft Crystal Structure of the Vault Shell at 9 Angstroms Resolution	9.00
2R7E	A,B	Crystal Structure Analysis of Coagulation Factor VIII	3.70
2W0C	A-T	X-RAY STRUCTURE OF THE ENTIRE LIPID-CONTAINING BACTERIOPHAGE PM2	7.00
2ZIX	A,B	Crystal structure of the Mus81-Eme1 complex	3.50
3A5C	A-P	Inter-subunit interaction and quaternary rearrangement defined by the central stalk of prokaryotic V1-ATPase	4.51
3A5D	A-P	Inter-subunit interaction and quaternary rearrangement defined by the central stalk of prokaryotic V1-ATPase	4.80
3B4R	A,B	Site-2 Protease from Methanocaldococcus jannaschii	3.30
3CTS	A	CRYSTALLOGRAPHIC REFINEMENT AND ATOMIC MODELS OF TWO DIFFERENT FORMS OF CITRATE SYNTHASE AT 2.7 AND 1.7 ANGSTROMS RESOLUTION	1.70
3CW2	A-N	Crystal structure of the intact archaeal translation initiation factor 2 from Sulfolobus solfataricus .	2.80
3DWW	A,B,C	Electron crystallographic structure of human microsomal prostaglandin E synthase 1	
3EOW	R	Poliovirus receptor CD155 D1D2	3.50
3FUS	A	Improved Structure of the Unliganded Simian Immunodeficiency Virus gp120 Core	4.00
3IJ2	A,B,X,Y	Ligand-receptor structure	3.75
3IKM	A,B,C,D,E,F	Crystal structure of human mitochondrial DNA polymerase holoenzyme	3.24
3K7A	A-M	Crystal Structure of an RNA polymerase II-TFIIB complex	3.80
3KGV	A-F,O-Y	Crystal Structure of Human DNA-dependent Protein Kinase Catalytic Subunit (DNA-PKcs)	6.60
3KRN	A,B	Crystal Structure of C. elegans cell-death-related nuclease 5(CRN-5)	3.92
1L6L	1-Z	Structures of Apolipoprotein A-II and a Lipid Surrogate Complex Provide Insights into Apolipoprotein-Lipid Interactions	2.30
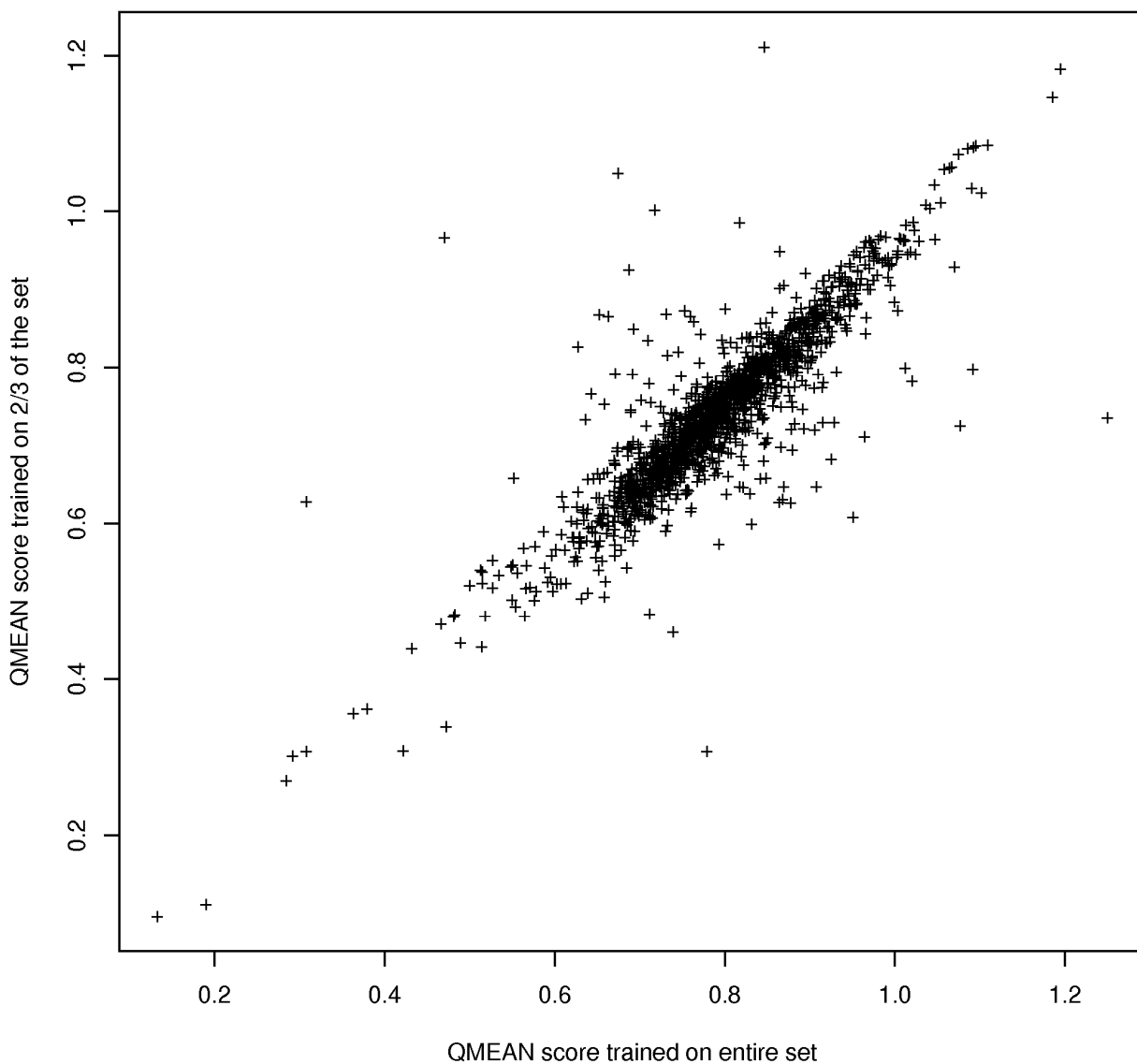
Figure S7: Cross-validation analysis on 1/3 of the training set (1523 chains). X-axis: QMEAN scores with potentials based on the original training set (i.e. test structures are part of training set to evaluate possible over-training); Y-axis: QMEAN scores with potentials trained on reduced training set (remaining 2/3, no overlapping structures).

Table S5. Proteins in the extended *biological unit reference set* with high QMEAN scores (Z-score > 3 standard deviations). From 26 structures with a QMEAN Z-score above 3 standard deviations 22 proteins are from thermophilic and hyperthermophilic organisms.

| PDB id	chains	Species/description	QMEAN Z-score
1GXJ	A,B	Thermotoga maritima	3.35
1M5Q	A-N	Pyrobaculum aerophilum	3.55
1TR8	A,B	Methanothermobacter marburgensis	3.10
1VKF	A,B	Thermotoga maritima MSB8	3.61
1W8S	A-J	Thermoproteus tenax	3.91
1XI3	A,B	Pyrococcus furiosus	3.18
1ZAV	A,U-Z	Thermotoga maritima	3.64
2BRX	A,B	Pyrococcus furiosus	3.37
2CU3	A,B	Thermus thermophilus HB8	3.60
2CW5	A-C	Thermus thermophilus	3.86
2GXQ	A,B	Thermus thermophilus HB27	3.32
2IEL	A,B	Thermus thermophilus	4.15
2NZC	A-D	Thermotoga maritima MSB8	3.10
2WG5	A-L	Archaeoglobus fulgidus	4.14
2Z8U	A,B	Methanococcus jannaschii	4.47
2ZZ2	A,B	Methanothermobacter thermautotrophicus	3.25
2ZZ3	A,B	Methanothermobacter thermautotrophicus	3.04
3A1D	A,B	Archaeoglobus fulgidus	3.56
3BYP	A,B	Thermus thermophilus	3.83
3CU9	A	Geobacillus stearothermophilus	3.03
3G1V	A,B	Methanothermobacter thermautotrophicus str. Delta H	3.09
3H43	A-L	Methanocaldococcus jannaschii	4.19
2AI4	A,B	Shewanella oneidensis MR-1 (MCSG)	3.71
3ESM	A	Nocardia farcinica (NYSGXRC)	3.04
1VJQ	A,B	Designed protein based on procarboxypeptidase-A	3.33
1N0Q	A,B	Designed consensus ankyrin repeat	4.57
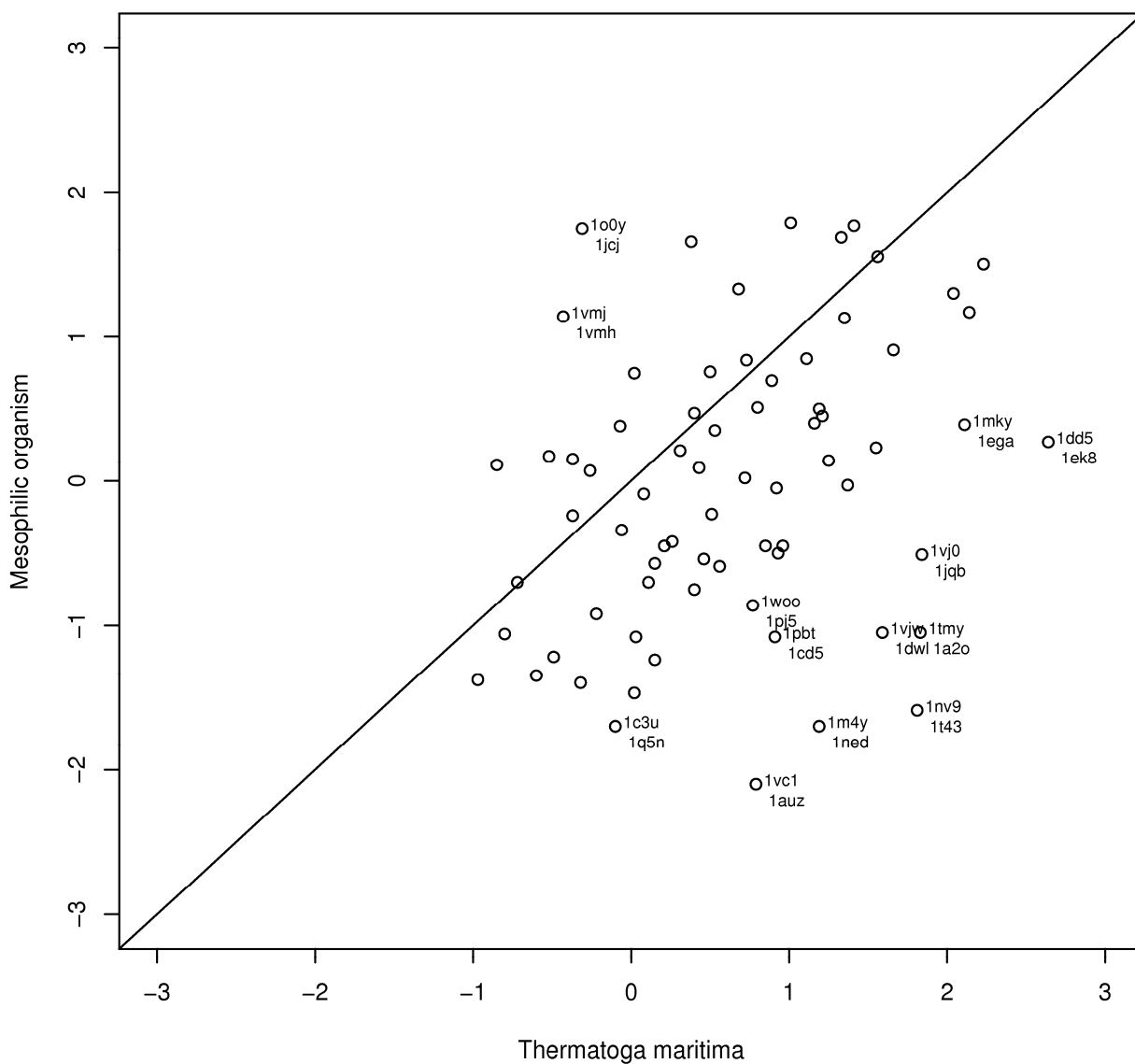
Figure S8: Direct comparison of the QMEAN Z-scores for 72 pairs of homologous proteins from *Thermatoga maritima* and their mesophilic counterparts. In 75% of the cases higher scores are assigned to the thermophilic proteins.

Table S6. Comparison of QMEAN based on normalized potentials (QMEANnorm) with single model scoring function of CASP8 on **easy targets** with mean GDT_TS of the top five models above 50. global r: correlation against GDT_TS over all model from all targets; mean r: per-target correlation coefficients averaged over all easy targets; mean ΔGDT_TS: average deviation of model with best score and best model. The statistical significance of the difference is measures with a paired t-test (p-values in italic mark significant differences).

group name	group id	#targets	global r	mean r	p-value	mean ΔGDT_TS	p-value
MULTICOM-REFINE	13	122	0.745	0.73	0.1306321	0.09	0.91019
GS-MetaMQAP	98	121	0.744	0.71	2.15E-005	0.13	*0.0062723*
QMEANnorm	-	122	0.742	0.74		0.09	
QMEANfamily	82	107	0.714	0.75	*0.0157545*	0.09	0.5256816
QMEAN	90	121	0.714	0.72	*0.0218905*	0.09	*0.0465433*
MULTICOM-CMFR	69	122	0.703	0.76	0.3241117	0.08	0.375808
circle	396	122	0.687	0.71	*0.002*	0.11	0.10
Bilab-UT	325	121	0.670	0.69	*4.37E-005*	0.11	0.20
SIFT_consensus	232	117	0.659	0.69	*1.22E-006*	0.11	0.10
MULTICOM-RANK	131	122	0.659	0.71	*0.0071145*	0.08	0.3830112
BMF_PP	146	96	0.655	0.61	*1.79E-013*	0.20	*0.0003*
ModFOLD	199	122	0.647	0.62	*2.66E-016*	0.14	*0.006269*
Fiser-QA	152	121	0.619	0.56	*1.11E-015*	0.19	*5.13E-006*
Pcons_ProQ	469	122	0.614	0.67	*1.53E-008*	0.13	*0.001*
MUFOLD-QA	245	122	0.588	0.65	*5.87E-009*	0.12	*0.0177344*
DistillSN	272	120	0.577	0.48	*5.26E-021*	0.21	*2.04E-011*
Fiser-QA-COMB	177	121	0.574	0.52	*2.92E-017*	0.23	*2.59E-007*
DISTILLF	117	118	0.550	0.65	*7.28E-010*	0.14	*0.003*
SIFT_SA	308	112	0.510	0.64	*7.09E-010*	0.11	0.1532306
SELECTpro	151	122	0.497	0.64	*6.81E-013*	0.15	*0.001*
MODCHECK-HD	94	122	0.474	0.30	*1.64E-033*	0.15	*7.35E-006*
Fiser-QA-FA	329	121	0.442	0.52	*9.62E-022*	0.19	*7.23E-006*
qa-ms-torda-server	109	117	0.071	0.06	*2.71E-037*	0.49	*4.76E-027*
ProtAnG_s	105	121	0.077	0.12	*3.23E-043*	0.14	*0.0005*

Table S7. Comparison of QMEAN based on normalized potentials (QMEANnorm) with single model scoring function of CASP8 on **hard targets** with mean GDT_TS of the top five models below 50. global r: correlation against GDT_TS over all model from all targets; mean r: per-target correlation coefficients averaged over all hard targets; mean ΔGDT_TS: average deviation of model with best score and best model. The statistical significance of the difference is measures with a paired t-test (p-values in italic mark significant differences).

| group name	group id	#targets	global r	mean r	p-value	mean ΔGDT_TS	p-value
MULTICOM-REFINE	13	122	0.72626	0.71	0.9101726	0.09	0.9301079
Bilab-UT	325	121	0.72522	0.68	0.2320285	0.11	0.4910312
MULTICOM-CMFR	69	122	0.68274	0.75	*0.0426145*	0.08	0.3509837
Pcons_ProQ	469	122	0.67651	0.66	*0.018169*	0.12	0.6577917
GS-MetaMQAP	98	121	0.67167	0.70	0.307868	0.12	0.300074
MULTICOM-RANK	131	122	0.67082	0.70	0.2737412	0.08	0.3258547
QMEANnorm	-	122	0.64856	0.72		0.09	
QMEAN	90	121	0.62054	0.71	0.9863701	0.09	0.8901362
DistillSN	272	120	0.60411	0.45	*2.26E-005*	0.18	*0.0194719*
DISTILLF	117	118	0.55304	0.61	*0.0315978*	0.14	0.0866024
QMEANfamily	82	107	0.54593	0.75	*0.004*	0.09	0.3342285
ModFOLD	199	122	0.50701	0.61	*2.22E-006*	0.12	0.0706222
circle	396	122	0.48673	0.71	0.9145004	0.10	0.7857503
SIFT_consensus	232	117	0.42824	0.68	0.1163783	0.10	0.4547869
MUFOLD-QA	245	122	0.42797	0.63	0.10	0.11	0.9167522
SIFT_SA	308	112	0.37872	0.60	*0.0333312*	0.11	0.2610832
BMF_PP	146	96	0.34419	0.61	*2.27E-005*	0.17	*0.0003*
SELECTpro	151	122	0.33682	0.62	*0.0246872*	0.14	*0.0102499*
Fiser-QA-COMB	177	121	0.24619	0.54	*1.05E-005*	0.19	*0.0003*
Fiser-QA-FA	329	121	0.2443	0.54	*1.41E-007*	0.17	*0.0280583*
Fiser-QA	152	121	0.23607	0.57	*0.002*	0.17	*0.003*
MODCHECK-HD	94	122	0.21415	0.34	*4.42E-009*	0.13	0.0706954
ProtAnG_s	105	121	0.01152	0.10	*5.35E-016*	0.13	0.4346289
qa-ms-torda-server	109	117	-0.0165	0.10	*3.71E-015*	0.38	*2.95E-007*
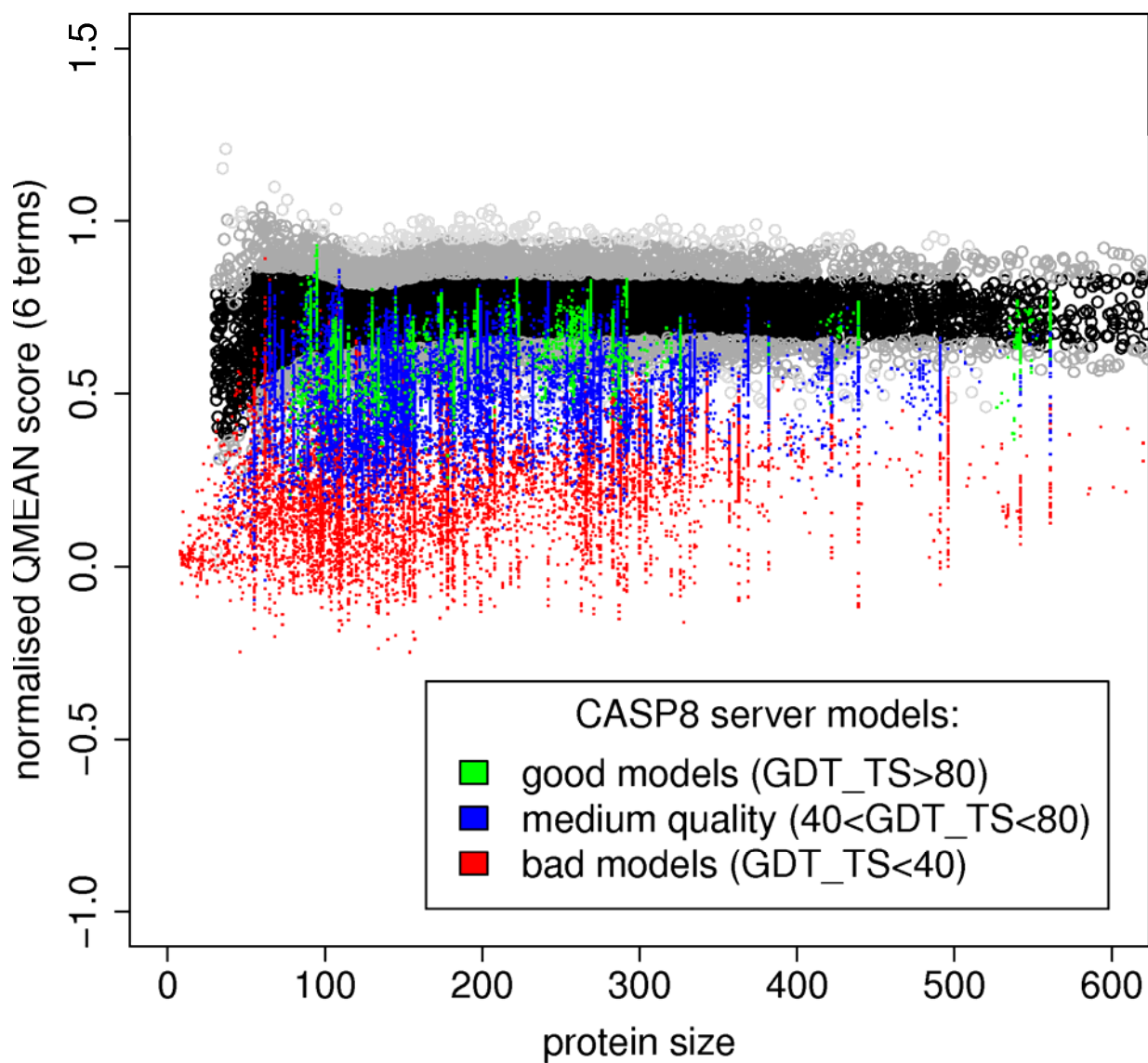
Figure S9: Analysis of theoretical protein structure models using nornmalised QMEAN scores. Scores for models from CASP8 are shown in relation to scores of experimental reference structures (black and gray). The models are split into three quality ranges with roughly random models in red, medium-quality models in blue and good models in green.
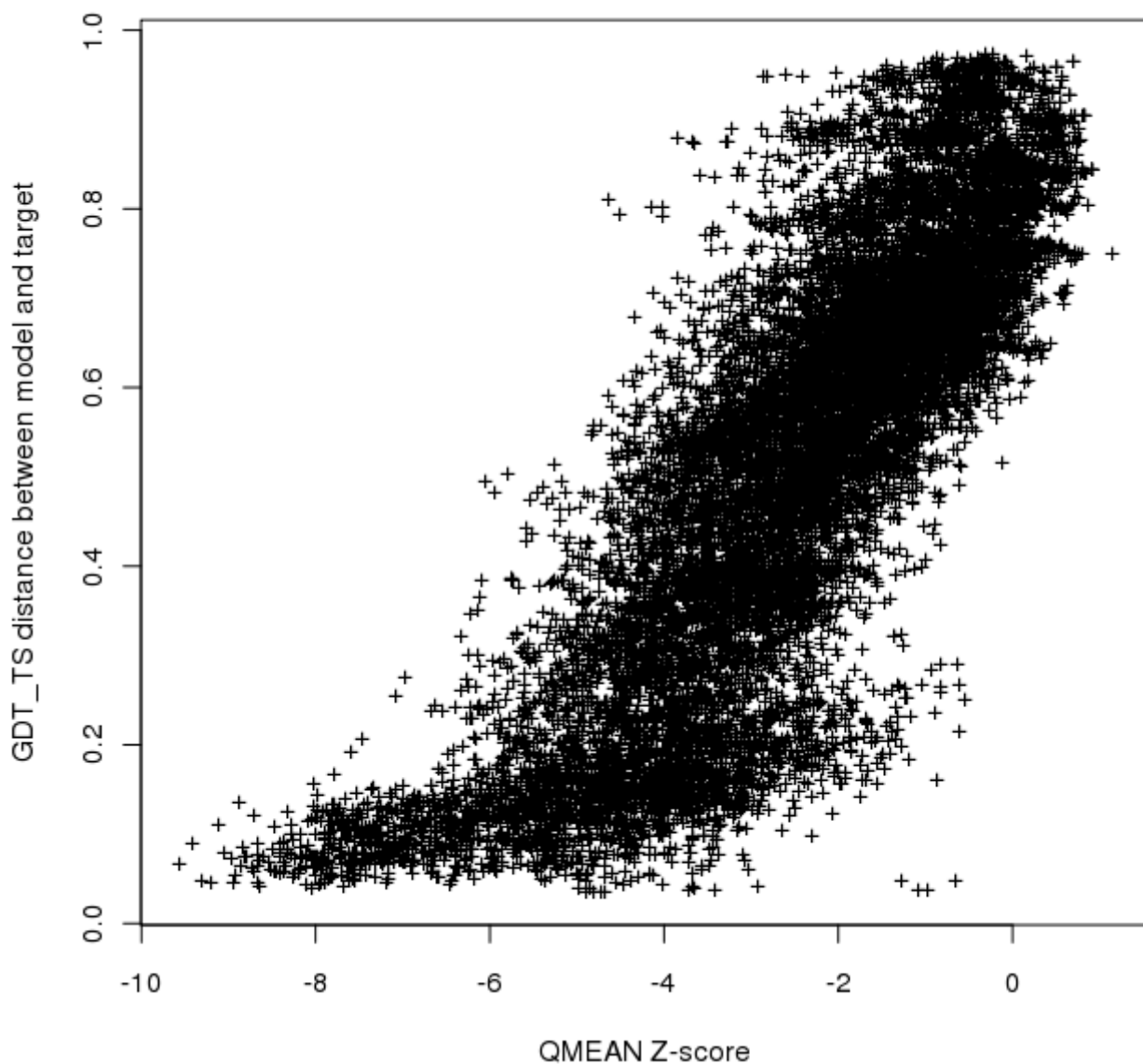
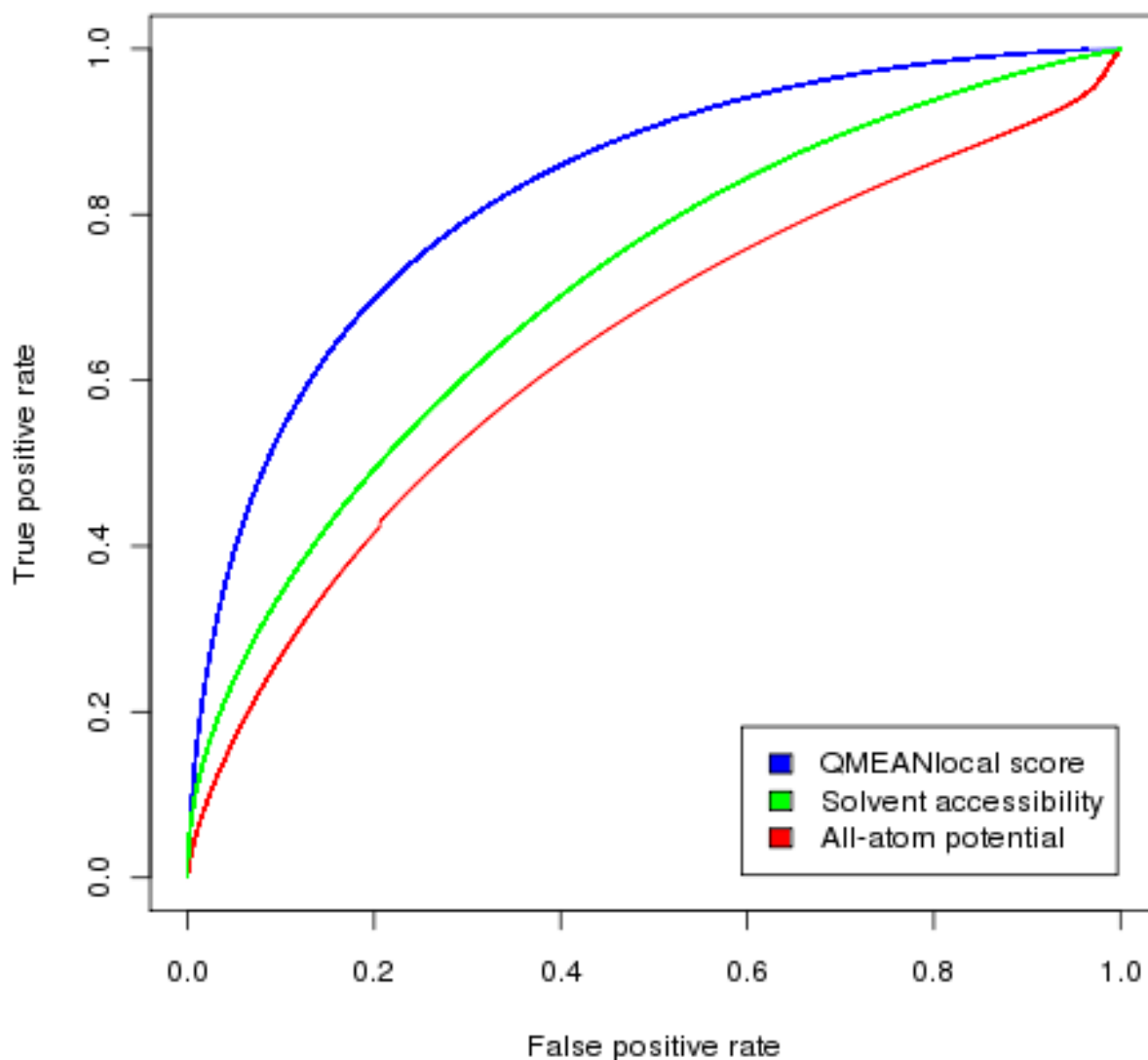**Figure S10**: Correlation between GDT_TS and QMEAN Z-score for CASP8 server models larger than 150 residues.
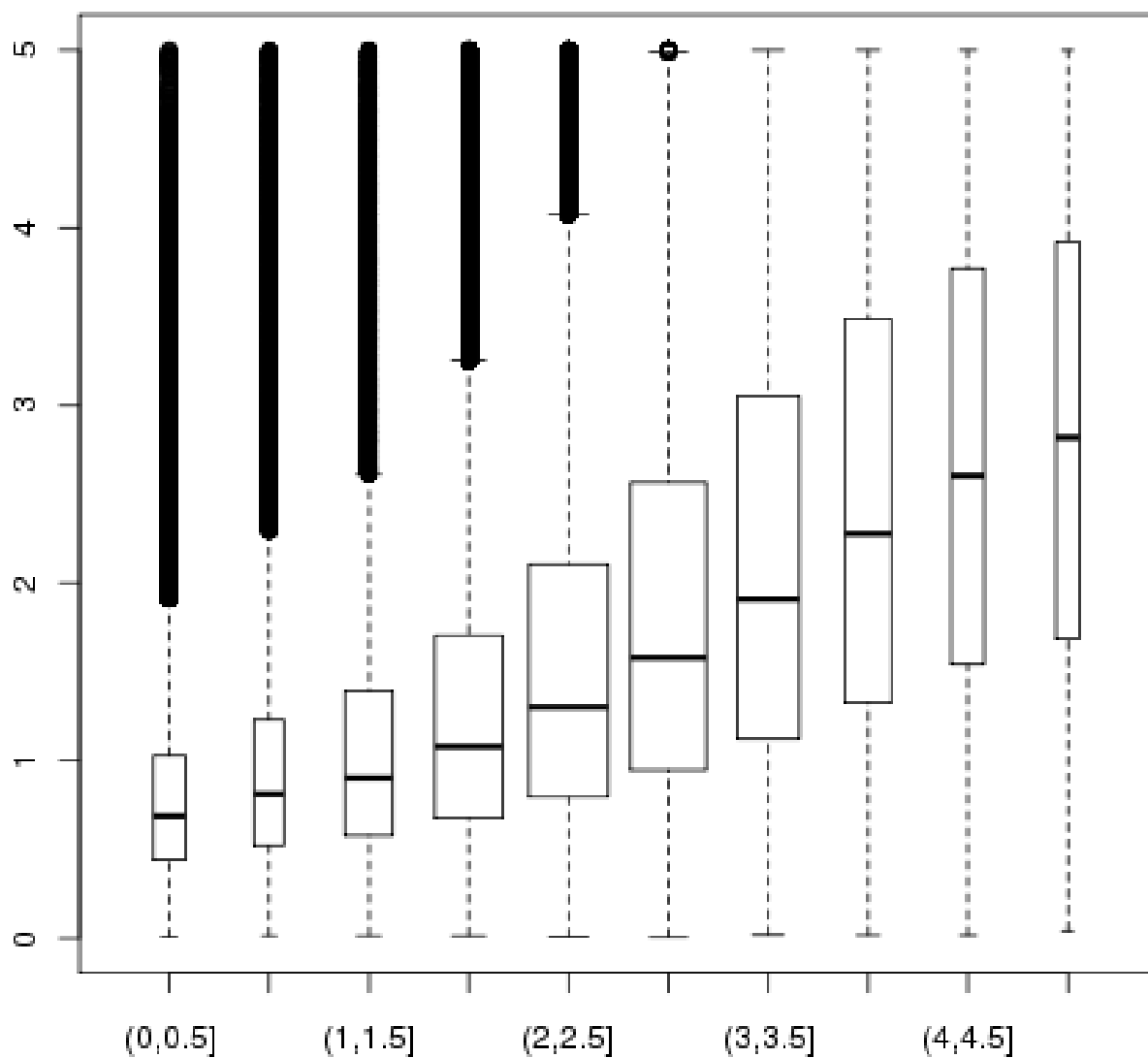
Figure S11: Boxplot analysis on all server models of CASP8: predicted local error based on QMEANlocal (x-axis) against the measured C-alpha deviation after rigid body superposition. The dataset was caped at 5 Angstrom. Only a rough correlation between predicted and calculated error is observed.

Figure S12: ROC curve analysis of all residues of all CASP8 server targets (~6.5 million residues) based on three local error estimates. The dataset is sorted by the error estimate and the each residue is classified as "true" (measured C-alpha distance to native < 2.5A) or "false" (>2.5A). The 10% lowest scoring residues according to QMEANlocal capture more than half of all residues in the set deviating by less than 2.5 Angstrom. The trivial measure "solvent accessibility" of a residue performs betters in distinguishing between good and bad that the all-atom terms. The integration of all 8 terms in QMEANlocal performs significantly better than all individual terms.